Quaternary Science Advances 2 (2020) 100013

Contents lists available at ScienceDirect

Quaternary Science Advances

journal homepage: www.journals.elsevier.com/quaternary-science-advances

2,200-Year tree-ring and lake-sediment based snowpack reconstruction for the northern Rocky Mountains highlights the historic magnitude of recent snow drought

Spruce W. Schoenemann [a,*], Justin T. Martin [b], Gregory T. Pederson [b], David B. McWethy [c]

[a] Environmental Sciences Department, The University of Montana Western, Dillon, MT, 59725, USA
[b] U.S. Geological Survey, Northern Rocky Mountain Science Center, Bozeman, MT, 59715, USA
[c] Earth Sciences Department, Montana State University, Bozeman, MT, 59717, USA

ARTICLE INFO

Keywords:
Holocene
Northern rocky mountains
Snowpack
Lake sediments
Tree-rings
Stable isotopes
Paleoclimatology

ABSTRACT

In recent decades, Rocky Mountain accumulated snowpack levels have experienced rapid declines, yet long-term records of snowpack prior to the installation of snowpack observation stations in the early and mid 20th century are limited. To date, a small number of tree-ring based reconstructions of April 1 Snow Water Equivalent (SWE) in the northern Rocky Mountains have extended modern records of snowpack variability to ~1200 C.E. Carbonate isotope lake sediment records, provide an opportunity to further extend tree-ring based reconstructions through the Holocene, providing a millennial-scale temporal record that allows for an evaluation of multi-scale drivers of snowpack variability, from internal climate dynamics to orbital-scale forcings. Here we present a ~2200 year preliminary reconstruction of northern Rockies snowpack based on $\delta^{18}O$ measurements of sediment carbonates collected from Foy Lake, Montana. We explore the statistical calibration of lake sediment $\delta^{18}O$ to an annually resolved snowpack reconstruction from tree rings, and develop an approach to assess and quantify potential sources of error in this reconstruction approach. The sediment-based snowpack reconstruction shows strong low-frequency variability in snowpack over the last two millennia with few snow droughts approaching the magnitude of recent snowpack declines. Given the growing availability of high-resolution, carbonate-rich lake sediment records, such reconstructions could help improve our understanding of how snowpack conditions varied under previous climatic events (mid-Holocene climate optimum ca. 9–6 ka), providing critical insights for anticipating future snowpack conditions.

1. Introduction

Snowpack in the western U.S. serves as an invaluable resource since it acts as a natural reservoir, historically providing the majority of annual runoff through consistent melt during the summer dry season (Bales et al., 2006; Barnett et al., 2008). However, over recent decades, reductions in the amount of total accumulated winter snowpack along with earlier spring melt-out timing (Barnett et al., 2008; Lundquist et al., 2008; Pederson et al., 2011b; Mote et al., 2018) has increasingly stressed municipal and agricultural water systems, terrestrial and aquatic ecosystems, and contributed to increased wildfire activity (Westerling et al., 2006). Continued rapid changes in western U.S. snow dynamics challenges the management of water resources, threatening important societal services including the generation of hydroelectricity and the maintenance of cold-water fisheries and winter recreation and tourism (Bales et al., 2006; Pederson et al., 2011b; Harpold et al., 2012, 2017).

Measurements of Rocky Mountain snowpack have historically been made on or around the first of April due to the generally strong relationship to total winter snowpack, and the utility for forecasting warm season streamflow (Bohr and Aguado, 2001). Reflecting the measurement's importance to water resources, snowpack has most commonly been recorded in units of inches (or millimeters) of snow water equivalence (the amount of water contained within the snowpack), or SWE. Over the past ~80 years, measurements of April 1 SWE have been made along repeat transects called snow courses, and from remote automated stations (i.e., Snow Telemetry or SNOTEL) for a network of major water contributing sites across the western U.S. by the Natural Resources Conservation Service (NRCS). A handful of the earliest April 1 SWE measurements began in the 1920s, but the majority of the historical snow course stations came online around 1950, with SNOTEL station

* Corresponding author.
E-mail address: spruce.schoenemann@umwestern.edu (S.W. Schoenemann).

https://doi.org/10.1016/j.qsa.2020.100013
Received 15 April 2020; Received in revised form 12 August 2020; Accepted 13 August 2020
Available online 22 August 2020

installations beginning in the late 1960s. Despite the density of modern SWE observations, most of these records are too short to evaluate key low- and high-frequency climate system forcings (e.g., changes in insolation as well as multi-decadal and inter-annual teleconnections including the Pacific Decadal Oscillation (PDO), Atlantic Multi-decadal Oscillation (AMO), and El Niño Southern Oscillation (ENSO) among others) associated with snowpack variability (Pederson et al., 2011b; Harpold et al., 2017).

Tree-rings have been successfully employed in reconstructing and extending observational records of April 1 SWE in a number of studies across the western U.S. (Woodhouse, 2003; Pederson et al., 2011b; Belmecheri et al., 2015; Barandiaran et al., 2017). Using different combinations of moisture-limited (i.e., low-elevation, cool season drought sensitive – positively snowpack correlated chronologies) and energy-limited (i.e., high-elevation, snow suppressed growth or spring temperature sensitive – negatively snowpack correlated chronologies) tree-ring chronologies, each of these prior studies demonstrated strong interannual through multidecadal-scale fidelity between reconstructions and modern-era snowpack data at spatial scales of medium to large watersheds (i.e., ~100–1000 km^2). The exact calendar-year dating accuracy combined with the seasonal to annual resolution of the tree-ring records allows for the highest potential cross correlation and time-resolution of any environmental proxy with hydroclimatic data. Indeed, tree-ring based SWE reconstructions for the major watersheds of the intermountain West have extended our long-term understanding of spatiotemporal variability in SWE to ~1200 C.E. (Pederson et al., 2011a). However, to obtain a multi-millennial perspective with the potential of capturing decadal to millennial-scale trends and variability in SWE requires the integration of lower temporal resolution paleoclimate archives that have the potential of spanning the mid-to-early Holocene (~8–12 ka).

Lake sediment cores are one of the few proxy archives that span multiple millennia, and have been shown to record changes in hydroclimate, fire, and vegetation (e.g., Whitlock et al., 2008, 2012; Brunelle et al., 2013; Anderson et al., 2015a). Depending on the sedimentation rate, quality of the depth-age model, and sampling frequency, lake sediments are capable of recording environmental variations with near-annual to decadal time resolution (Power et al., 2006; Stevens et al., 2006; Stone and Fritz, 2006; Anderson, 2012). This common overlap in the temporal resolution of dating accuracies and retained frequencies of hydroclimatic variability between tree-ring and high-resolution lake sediment records presents a unique opportunity to statistically calibrate, estimate uncertainty, and extend tree-ring reconstructions of snowpack that are anchored to modern conditions.

Additionally, in high-elevation locales, snowmelt is likely to be the dominant influence on isotopic values recorded in lake archives, and therefore may be suitable as a reconstruction target for carbonate-rich lakes (Anderson et al., 2016a). In the Rocky Mountain region of western North America, the majority of precipitation (60–70%) falls as snow during the months from October to May (Pederson et al., 2011b; Anderson et al., 2016a). During the spring, this stored precipitation melts yielding surface runoff, soil moisture, and groundwater recharge. The isotope ratios of these snow-based water sources, rather than rainfall, tend to be integrated into terrestrial climate proxies such as lake sediment $\delta^{18}O$ (e.g., Anderson, 2012), stalagmites (e.g., Lundeen et al., 2013), and even tree cellulose (e.g., Berkelhammer and Stott, 2012).

To improve our understanding of snowpack variability and its

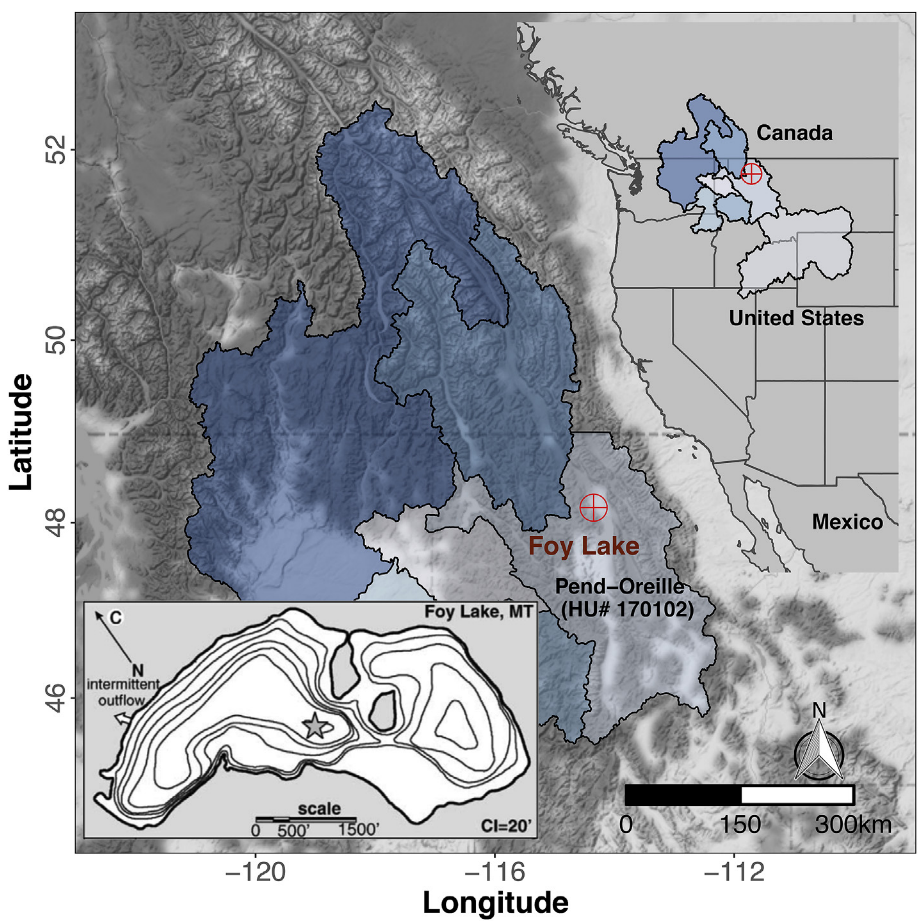

Fig. 1. Study area map. (a) The location of Foy Lake, MT (red circle/cross) within the Pend Oreille Hydrologic Unit (HU) level-6 watershed (light blue), and **(b)** locator map of the domain of the Northern Rocky Mountains Snow Water Equivalent (NRM-SWE) reconstruction, **(c)** inset of bathymetric map of Foy Lake and sediment core position (star).

response to long-term climatic forcings, we develop methods for the statistical calibration of high-resolution lake sediment records to tree-ring based snowpack reconstructions. Specifically, we utilize the stable water isotope ratios of precipitation that are preserved in the carbonates of lake sediments from Foy Lake, Montana (Fig. 1) (Stevens et al., 2006; Stone and Fritz, 2006), along with the tree-ring based reconstructions of April 1 SWE for the northern Rockies (Pederson et al., 2011b) to: 1) develop a multi-millennial snowpack reconstruction by; 2) improving the accuracy of the lake sediment record depth-age model, 3) statistically calibrating the lake snow signal to existing tree-ring records, and 4) quantifying the dominant hydroclimate sensitivity of the carbonate oxygen isotope ratios.

In doing so, this research provides a novel methodological approach with potential broad application for the statistical calibration of high-resolution lake sediment records to tree-ring based climate reconstructions where they co-occur. Additionally, these methods help improve our understanding and interpretation of the climate signal recorded in the isotope proxy archives (e.g., Evans et al., 2013; Jones et al., 2016a), while more than doubling the length of the existing northern Rockies snowpack reconstructions from Pederson et al. (2011a). The new April 1 SWE reconstructions provide an important long-term context and understanding of drivers of snowpack variability over the Common Era (C.E.).

2. Methods

2.1. Identifying potentially suitable snowpack-dominated lake sediment cores

There are three key criteria for identifying candidate lakes for sediment coring and/or correlation-based dating and hydroclimatic analyses. The first is that the lake is located within a region of considerable annual snowfall. The greater the winter-season contribution of snowmelt to the annual lake water-balance, the more likely that the δ^{18}O signal preserved in the carbonates will reflect variations in winter temperature, precipitation, and/or the combined temperature and precipitation signal integrated in accumulated snowpack. The second criterion is that the lakes must have in-situ (i.e., authigenic) carbonate production to preserve an oxygen and carbon isotope record. The third criterion is that the sediment record must have annual to decadal temporal resolution for comparison against tree-ring reconstructed climate or other annual to near-annual resolution climate proxies. In this study we chose to test our quantitative reconstruction approach on the Foy Lake sediment core from northwestern Montana since it meets the above criteria and is an existing high-resolution, carbonate-bearing sediment core located in the northern Rocky Mountains (Stevens et al., 2006; Stone and Fritz, 2006) (Fig. 1).

2.2. Foy Lake sediment δ^{18}O record

A 2200-year long record of δ^{18}O in sediment carbonates from Foy Lake in northwestern Montana was collected by Stone and Fritz (2006) and further developed by Stevens et al. (2006) (Fig. 2). The resolution of the record over this period is approximately five years. Settlement of the region and the construction of a lumber mill that included impoundment of the lake, is thought to have influenced the level of δ^{18}O in Foy Lake carbonates after 1890, resulting in a consistent shift to lower δ^{18}O levels on an annual basis due to greater through-flow. Stevens et al. (2006) suggest the record is sensitive to both precipitation and temperature dynamics based on significant correlations with both regional Palmer Hydrologic Drought Index (PHDI), and a nearby tree-ring based reconstruction of precipitation spanning 700 years.

2.3. Northern Rocky Mountains April 1 snow water equivalent (NRM-SWE) reconstruction

An 800-year long record of April 1 SWE for the northern Rocky Mountains was developed by Pederson et al. (2011b) using a network of moisture and energy-limited tree-ring records from across the Western U.S. and Canada (Fig. 1). The record is annually resolved and skillfully captures the inter-annual to multi-decadal scale variability in snowpack development for the watershed including Foy Lake. The record overlaps the pre-settlement period (1252–1890 C.E.) of the Foy Lake δ^{18}O record, and the full lake record to 1992 C.E. The instrumental portion of the record was comprised of NRCS snow course and SNOTEL records aggregated across the 10 USGS level 6 hydrologic units (HU) including HU 170102 – Pend-Oreille watershed which encompasses Foy Lake (Fig. 1) (Pederson et al., 2011b).

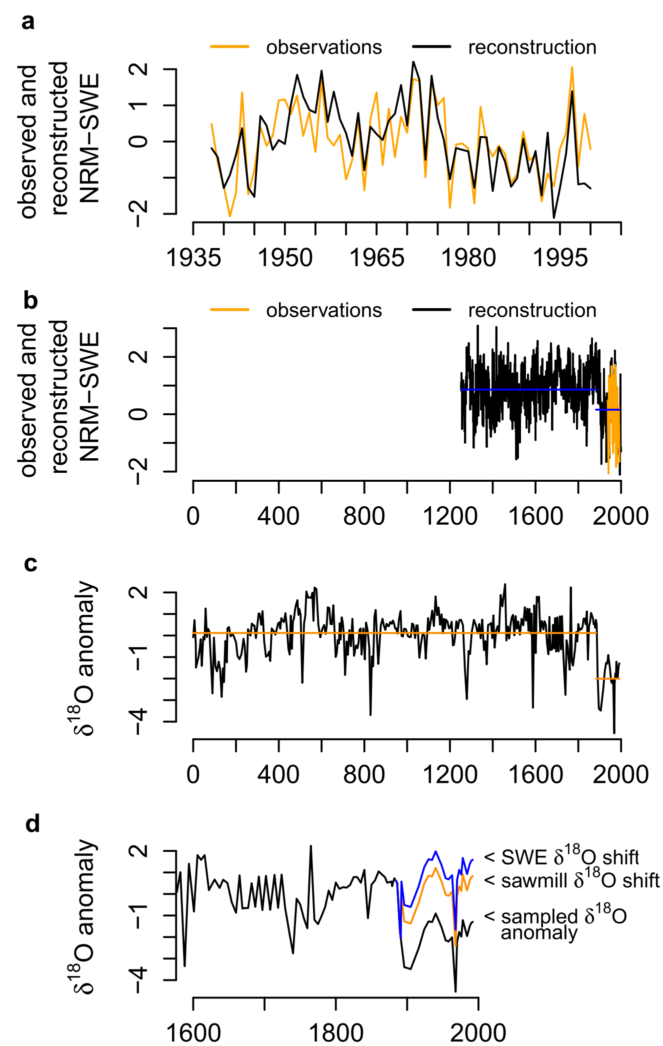

Fig. 2. Northern Rockies snowpack and Foy Lake sediment δ^{18}O. (a) The observed and reconstructed April 1st snow water equivalent (SWE) anomaly for the northern Rocky Mountains showing the period common to both records **(b)** The observed (1936–2006) April 1st snow water equivalent (SWE) anomaly overlaid on the 800-year long tree-ring based reconstruction of northern Rockies SWE, **(c)** the 2200 year ~5yr resolution Foy Lake sediment δ^{18}O record, **(d)** and the last 400 years of the Foy Lake sediment δ^{18}O record showing the adjustment made to the δ^{18}O values after 1890 to reflect human alteration of the lake chemistry and the expected shift in δ^{18}O values due to changes in northern Rockies SWE during that time period.

2.4. Visually refining the dates of the Foy Lake δ^{18}O record using the NRM-SWE reconstruction

Unlike tree-ring records in which the formation dates of annual rings can be correctly dated to calendar-year accuracy using the visual and statistical process of cross-dating (Stokes and Smiley, 1968), considerable uncertainty exists in estimating the deposition date of particular layers (or at specific depths) within a lake sediment core (Ramsey, 2008; Parnell et al., 2011). In the case of the Foy Lake record, the most recent radiocarbon estimated date from the core is for the year 1106 C.E. ± 35 years, based on ^{14}C in wood at a depth of 87.3 cm. As a result, there are no radiocarbon dates within the overlapping period between the lake sediment and tree ring records (1252–1992 C.E.) that could be useful for aligning the two records in time. However, the observed correlations between Foy Lake $\delta^{18}O$ and PDHI (Stevens et al., 2006) suggests: 1) that the dating of the Foy Lake record is generally robust over this time period, and 2) that $\delta^{18}O$ in Foy Lake sediment record may exhibit a snow or moisture balance climate sensitivity similar enough to the tree-ring reconstructions that it is possible to further correct the accuracy of the dating using identified extreme event anomalies. This approach is similar to methods used in visually cross-dating individual tree-ring series at a site and builds directly on the approach used by Chellman et al. (2017) to correct the dating of the Fremont Glacier ice core water isotope record against a local tree-ring chronology.

Because snowpack $\delta^{18}O$ and SWE are known to be negatively correlated in the northern Rockies (Anderson et al., 2015b), it is possible to align the Foy Lake $\delta^{18}O$ record with the NRM-SWE record by matching the patterns in the records themselves via approaches from Chellman et al. (2017), rather than trying to align the records using radiocarbon based depth-age model dating that contain considerable dating uncertainty (Prell et al., 1986; Shackleton et al., 1995). To test this, we first confirmed that the Foy Lake $\delta^{18}O$ record was significantly negatively correlated with NRM-SWE over the common undisturbed period of both records (1252–1890 C.E.). To match the resolution of the NRM-SWE record to the sample resolution of the lake before correlating the records, values in the NRM-SWE reconstruction were first binned in 5-year bins centered on the estimated formation year of each lake sediment sample (each sample = 1 cm thick layer). NRM-SWE and the raw unadjusted Lake $\delta^{18}O$ values were significantly negatively correlated with $r = -0.22$ ($p = 0.012$) based on Pearson's product-moment correlation, and $rho = -0.21$ ($p = 0.016$) based on Spearman's rank correlation. Next, to facilitate visual pattern matching of the extreme anomaly events, we standardized both records by subtracting their means and dividing by their standard deviation converting them to *z*-scores. Given the NRM-SWE records negative correlation with lake $\delta^{18}O$, the sign of the SWE record was reversed (i.e., multiplied by −1) to facilitate comparison.

Since the temporal resolution of the Foy Lake $\delta^{18}O$ record is approximately five years while the NRM-SWE time series is annually resolved (Fig. 1), we used a linear interpolation approach to infill missing values in the $\delta^{18}O$ record. Then to make the records directly comparable, we smoothed them with a 20-year cubic smoothing spline to reduce the complexity of the patterns in the time series for visual pattern matching (Cook and Kairiukstis, 1990; Gray et al., 2017) (Fig. 2a).

This approach best increased the strength of the common signal in both records relative to the noise that may be associated with more localized climate or biophysical influences unique to each record. This is because the climatic processes that control decadal to multi-decadal scale variability in snowpack tend to operate at large spatial scales – meaning that their influence should be consistently integrated into the regional climate signal at Foy Lake and within the NRM-SWE record. Plotting the

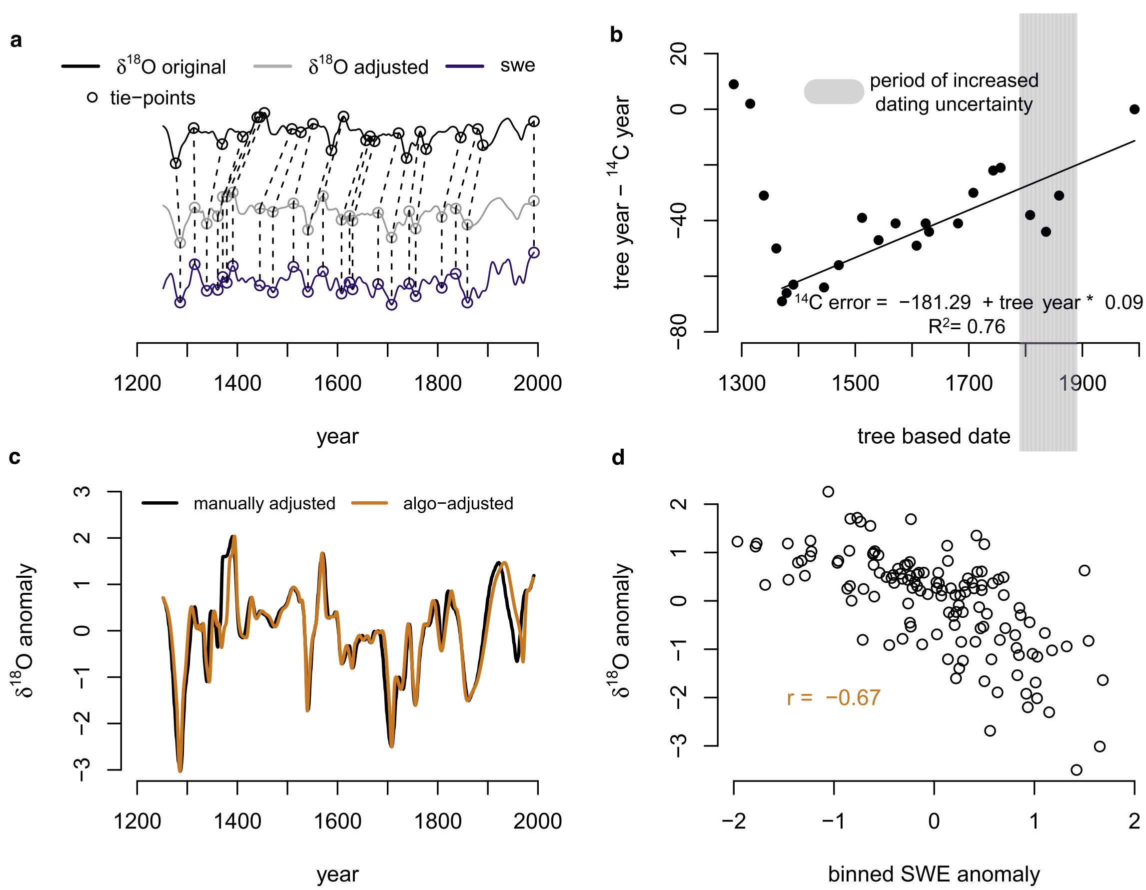

Fig. 3. Dating corrections of the Foy Lake isotope record. (a) The uncorrected and corrected Foy Lake $\delta^{18}O$ record and Northern Rocky Mountains Snow Water Equivalent (NRM-SWE) reconstruction showing tie points used to match the $\delta^{18}O$ record to the NRM-SWE record, **(b)** the difference between the tree-ring corrected lake sediment date (tree year) and the ^{14}C estimated sediment date (^{14}C year) for the tie points shown in panel a, **(c)** the twenty-year splines of manually-adjusted and algorithmically adjusted lake sediment $\delta^{18}O$ anomaly records, **(d)** five year binned values of NRM-SWE vs. corrected lake sediment $\delta^{18}O$ anomalies.

$\delta^{18}O$ record beside the NRM-SWE record revealed obvious similarities in the low-frequency dynamics and decadal anomalies (Fig. 3a). To visually align these patterns in time, those points shown in the $\delta^{18}O$ record in Fig. 3a were assigned the tree-ring derived dates of the associated points found in the NRM-SWE record. Minor high and low anomalies in the records falling between these initial major tie points were then visually aligned by assigning the NRM-SWE dates to highs and lows in the $\delta^{18}O$ record in chronological order.

2.5. Algorithmic dating adjustment of $\delta^{18}O$ to NRM-SWE

The process of visually dating the climate-derived patterns in the lake $\delta^{18}O$ record to NRM-SWE is deeply rooted in the rigorously tested dendrochronological process of cross-dating tree-ring data (Stokes and Smiley, 1968) and is well supported by countless dendrochronological studies (Douglass, 1935; Fritts, 1976; Briffa et al., 2002). Recently, advances in automation of signal correlation using dynamic programming techniques now make it possible to match common signals in paleoclimate records algorithmically as well (Lisiecki and Lisiecki, 2002). We utilized the MATCH dynamic programming software for automatic correlation of the lake $\delta^{18}O$ to NRM-SWE to test whether an automated signal correlation technique would arrive at the same solution as that determined by visually "cross-dating" the records. The MATCH algorithm has several useful characteristics in that it preserves the sequence of events in each series by utilizing a monotonically increasing mapping function, and it allows control of reasonable accumulation rates in paleoclimate records by way of adjustable parameters (default parameters were used in this study) (Lisiecki and Lisiecki, 2002).

2.6. Correcting for anthropogenic changes in Foy Lake $\delta^{18}O$

As noted by Stevens et al. (2006), the Foy Lake $\delta^{18}O$ record spans two distinct time periods. Prior to European settlement of the region (200 B.C.E. to C.E. 1890), lake $\delta^{18}O$ averaged −4.4‰ but dropped abruptly after settlement to −6.2‰ (Fig. 2c and d). This change of 1.8‰ has been attributed to a reduced residence time of lake water associated with sawmill activities at the lake outlet beginning as early 1884 (Stevens et al., 2006; Power et al., 2011). However, at nearly the same time (~1905), average annual values of NRM-SWE also shifted abruptly lower (Fig. 2b). Given our finding that decreased NRM-SWE is associated with increased $\delta^{18}O$ in Foy Lake, it is likely that the 1.8‰ estimate of anthropogenic change in oxygen isotope levels is underestimated. This is because, in the absence of human modification of the lake hydrology, lake $\delta^{18}O$ post 1890 would have likely been higher than the long-term average due to a persistent decrease in NRM-SWE, the mean of which from 1890 CE to 1992 CE was 0.76 standard deviations (σ) lower than that of record prior to 1890 CE. Pre vs. post settlement $\delta^{18}O$ correlations with binned NRM-SWE (0.67 vs. 0.48 respectively) suggest lake $\delta^{18}O$ remained closely linked to snowpack development after settlement of the region. Considering this, it is likely that the lake $\delta^{18}O$ values after 1890 CE were proportionally higher as well. However, assuming such a shift occurred, it was clearly masked by anthropogenic changes to the lake hydrology that drove isotope levels lower.

To account for these changes in the oxygen isotope record, we first added the difference between the pre- and post-settlement $\delta^{18}O$ means (2.12 σ) to the $\delta^{18}O$ anomaly record. We then added a further 0.76 σ to the record to account for the negative shift in NRM-SWE over the same time period that was not accounted for in the original estimate of the anthropogenic influence on $\delta^{18}O$ by Stevens et al. (2006) (Fig. 2d). Doing so allows the most recent years of the $\delta^{18}O$ record to be included in calibrating the reconstruction model to the target NRM-SWE time series over the period of time when the reconstruction is most skillful.

2.7. Instrumental period correlations between snowpack, temperature, precipitation, lake sediment $\delta^{18}O$, and atmospheric circulation

After refining the dates of the Foy Lake sediment record, we examined the pairwise relationships between Foy Lake sediment $\delta^{18}O$, April 1 SWE, and warm-season (Mar–Aug) average temperature and cool-season (prior Nov–Mar) total precipitation records for the Pend-Oreille watershed (HU 170102) from the **P**arameter-elevation **R**egressions on **I**ndependent **S**lopes **M**odel (PRISM) (PRISM Climate Group, Oregon State University, http://www.prism.oregonstate.edu). The period of analysis spanned from 1900 to 1992 which is the most recent date of the Foy Lake $\delta^{18}O$ record. We obtained the April 1 SWE record from observational records that spanned 1937–1992 and reconstructed from tree-rings over the period 1900–1936 (Pederson et al., 2011b).

Twenty Foy Lake $\delta^{18}O$ measurements from carbonate sediments span the period from 1900–1992. In order to align the temporal resolution of the isotope and climate data, annual values of temperature, precipitation, and SWE were averaged into 5-year bins centered on the corrected formation date of each of the $\delta^{18}O$ values, resulting in twenty, roughly evenly spaced, climate and lake measurements over the 20th century. With the exception of 5 recent samples (containing a single overlapping year each) in the more intensively sampled top portion of the core, 20th century data in the 5-year bins do not overlap. Thus, we do not expect correlations of binned values to be significantly affected by unwanted autocorrelation associated with smoothed data. Rather, the correlations reported should generally reflect the relationship between lower frequency dynamics in regional hydroclimate and lake chemistry and accordingly should not be assumed to represent higher frequency hydroclimate and lake chemistry dynamics operating at interannual timescales.

To examine the circulation patterns responsible for the modern relationships between April 1 SWE and $\delta^{18}O$ at Foy Lake, we utilized the Hybrid Single-Particle Lagrangian Integrated Trajectory (HYSPLIT) model (Stein et al., 2015) which is a proven tool for investigating relationships between air parcel trajectories and resulting precipitation isotopic compositions (e.g., Sinclair et al., 2011; Bershaw et al., 2012). We used the NCEP/NCAR Reanalysis I climate data (http://www.esrl.noaa.gov/psd/) for the HYSPLIT climatological input. For the Foy Lake site, we calculated 5-day back trajectories at 6-hr intervals for the 1948–2019 analysis period. The 5-day duration is sufficient, in most cases, to trace trajectories to their Pacific moisture source. We limited our analysis to storm trajectories that precipitated (>20 mm/day) above the Foy Lake site and initiate the trajectory start height at 1500 m, which is representative of trajectory pathways over the 1–2 km altitude that incorporates the atmospheric level where most water vapor is advected (Bershaw et al., 2012). Since the dominant precipitation period for snowpack in northwest Montana is winter/early spring, we selected only prior November–March trajectories for analysis rather than the entire water year. To identify the spatial patterns of air parcel trajectory pathways we used the HYPSLIT clustering algorithm which calculates the total spatial variance explained based on the number of clusters and then bins all similar pathways into single trajectories along with its percentage of the total. In the case of Foy Lake, a total of 5 clusters best captured the spatial variance.

2.8. Reconstruction model development

NRM-SWE was modeled from Foy lake $\delta^{18}O$ using simple linear regression. We first examined the relationship between lake $\delta^{18}O$ and binned NRM-SWE via scatterplot (Fig. 3d) and found the relationship to be slightly curvilinear. Further exploration revealed lake $\delta^{18}O$ to be slightly negatively skewed while NRM-SWE was normally distributed. Considering this, we first transformed lake $\delta^{18}O$ to be approximately normally distributed using a maximum likelihood-estimated power transformation (Box and Cox, 1964). This transformation produced a linear relationship between lake $\delta^{18}O$ and binned NRM-SWE, as well as constant variance of model residuals. Because the bin width (5 years) used to bin SWE values around lake samples was typically less than the interval between lake samples ~5–7 years, autocorrelation within both lake $\delta^{18}O$ and binned NRM-SWE values is expected to be minimal except for that which is a shared reflection of low frequency climate dynamics in both variables intentionally retained in the model.

Because a simple regression reconstruction inherently underestimates the variability of the past due to a certain amount of unexplained variance in each regression model, we followed the standard approach (Lutz et al., 2012) to restoring the variance in the binned NRM-SWE record to the reconstruction. Error bounds for each year of the reconstruction were determined as the 95% prediction interval for modeled SWE using the delta method (Dorfman, 1938) and were proportionally scaled to match variance adjustments made to the reconstruction.

Finally, recall that the dating of the Foy lake $\delta^{18}O$ record was refined using the certain annual dating of the tree-ring based SWE reconstruction. Because this date refinement only extends back to 1252, any dating errors inherent to the earlier Foy lake $\delta^{18}O$ record also exist in the first 1400 years of the lake sediment based SWE reconstruction. Thus, being a hybrid tree-lake SWE reconstruction, the record itself is also characterized by a mix of uncertainties reflecting the estimated dating and reconstructed value accuracy of the original proxies used in its development. On average, the dating of the Foy lake $\delta^{18}O$ record was quite accurate in the sequential sense except for a brief and rapid change in sedimentation rates between ^{14}C-based age estimates (e.g., present day to ca 1106 C.E., the first radiocarbon date from the lake core). We have no reason to expect the dating accuracy of the earlier (prior to 1252 C.E.) Foy lake $\delta^{18}O$ record to be significantly different from recent portion where the average annual dating error was less than 40 years over the full 800-year record.

2.9. Cross-validation of reconstructed NRM-SWE

We performed cross-validation of model performance using a split-sample approach with an initial calibration period consisting of the earlier half of the NRM-SWE record and a verification period consisting of the latter half. Cross-validation was then run in reverse by switching the time periods used for calibration and verification. The statistics from each run are provided. We calculated the coefficient of determination (R^2) for the NRM-SWE record explained by the model parameterized only on training data (VRSQ) and did the same for the predictions made using all target data in the calibration of the model (CRSQ). Following standard methods, we also calculated the reduction of error statistic (RE) (Fritts, 1976) and the coefficient of efficiency (CE) (Briffa et al., 1998) for the reconstruction model.

3. Results

3.1. Visual and algorithmic dating corrections of the Foy Lake sediment $\delta^{18}O$ record

The visual and algorithmic cross-dating of the Foy Lake $\delta^{18}O$ indicated the need for an adjustment generally characterized by a simple shift to the entire $\delta^{18}O$ time series (Fig. 3a). This shift increased the strength of the correlation between $\delta^{18}O$ and SWE substantially from −0.21/−0.22 using the original ^{14}C-based dating to −0.66/−0.68 ($p < 0.001$) based on both Pearson and Spearman correlation measures respectively. This suggests that the overall pattern generating such a high correlation to SWE is inherent to the depth sequence of $\delta^{18}O$ in the lake sediments and is initially only obscured by a general offset in the ^{14}C-based dating of the original record. Assuming the $\delta^{18}O$ based adjustments more accurately estimate the dates in the Foy Lake record, then the original dates underestimated the age of the sampled sediment layers by approximately 30–70 years from circa 1400–1900, with underestimation increasing linearly with depth (Fig. 3b). An abrupt shift in the bias of the original depth-age model is then suggested during the transition from the periods associated with the Medieval Climatic Anomaly (MCA, ~800–1200 C.E.) to the Little Ice Age (LIA, ~1400–1850 C.E.). This suggests that the age model used to date the Foy Lake record from the top of the sediment core to the first ^{14}C date at 87.3 cm (ca 1106 C.E.) failed to capture changing rates of sediment deposition in Foy Lake due to the lack of additional dateable material present within the core within that time interval. Consequently, over that time period a substantial increase in sedimentation during the 14th century was not accounted for, which further offset the dating errors in the $\delta^{18}O$ record. Fig. 3a and c shows the 14th century sedimentation event and other differences between the original ^{14}C-based dates and those adjusted to the NRM-SWE record at each tie point.

A comparison of the age model adjustments from the MATCH algorithm to those made visually showed similar results, further supporting the validity of the adjusted chronology. Importantly, visual adjustments were first made to the Foy Lake $\delta^{18}O$ record before employing the automated technique because of the potential to bias corrections if the algorithm-based adjustment was performed first. The result was a very close match between the two adjusted time series showing a correlation of 0.82 between the manually adjusted and algorithmically adjusted record (Fig. 3c). The period of overlap between the algorithmically adjusted lake $\delta^{18}O$ record and SWE (1252–1990) is similar to that of the manually adjusted record (1252–1992) as is the maximum number of years made in the adjustment (69 years for both methods). The post-adjustment correlation of the lake $\delta^{18}O$ record with binned NRM-SWE using the MATCH algorithm was −0.67 ($p < 0.001$) while the manual adjustment also resulted in a correlation of −0.67 ($p < 0.001$). It is worth emphasizing the rather exceptionally high variance (0.45 R^2) shared by these two independent proxy records that are both recording fluctuations in SWE, albeit with varying amplitudes. Fig. 4 shows the full date-corrected lake $\delta^{18}O$ record as well as the NRM-SWE record and depicts both records in their original temporal resolutions along with the interpolated and/or smoothed timeseries.

3.2. Correlations between modern climate variables and δ18O

To establish the modern relationships between April 1 SWE, precipitation, temperature and lake $\delta^{18}O$, correlations between all variables were performed using both Pearson and Spearman correlation methods over the period of 1900–1992. As shown in Fig. 5, a statistically significant positive relationship exists between cool-season (prior Nov–Mar) precipitation and April 1 SWE ($r = 0.72/0.73$), while $\delta^{18}O$-SWE show a significant negative relationship ($r = -0.49/-0.59$) for Pearson and Spearman correlations, respectively. The cool-season temperature-SWE relationship is also negative, as expected, but only weakly correlated ($r = -0.17/-0.12$) (Fig. 5). Correlations between warm-season (Mar–Aug) temperature and SWE are somewhat higher though still not significant at the 95% confidence level ($r = -0.40/-0.43$). Correlations between warm season temperature and lake $\delta^{18}O$ are weak and insignificant at ($r = 0.25/0.16$).

3.3. Air parcel back-trajectories inform circulation patterns for anomalous SWE years

In order to better understand how regional circulation patterns contributed to the lake $\delta^{18}O$ and April 1 SWE relationship both spatially and temporally we compared air-parcel trajectories with the lake $\delta^{18}O$ and April 1 SWE records. Years that exhibited anomalous (≥1 σ) SWE values based on the instrumental SWE record (1937–2011) from Pederson et al. (2011b) were selected for air-parcel back-trajectory. Over the period of available re-analysis data (1948–2019 NCEP-NCAR Reanalysis I, from (Kalnay et al., 1996)), individual years with low SWE (n = 10) and high SWE (n = 14) were identified, and of these the 10 most recent high SWE years were chosen to provide an even comparison of total number of trajectories (Fig. 6). The air parcel back-trajectories show that in high SWE years there are ~45 more snow days than the low SWE years, a 22%

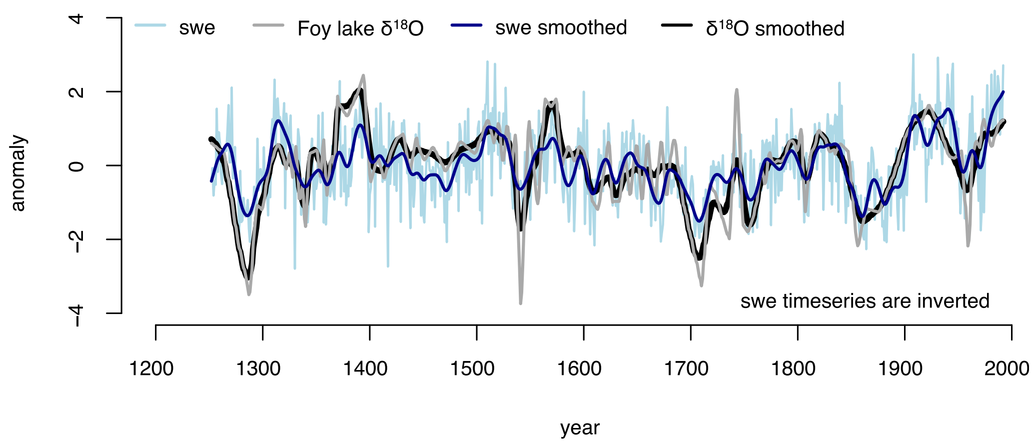

Fig. 4. Climate and Lake records. The reconstructed annual time series of Northern Rocky Mountains Snow Water Equivalent (NRM-SWE) and Foy Lake sediment δ^{18}O (~5 year resolution) overlain by the 20-year splines of Foy Lake sediment δ^{18}O and NRM-SWE. Both SWE timeseries are inverted. Note the high correlation of these independently based paleo-records is −0.67 (or 0.45 R^2).

increase on average. Clustering of these same back-trajectories found that high SWE years have moisture source origins in the far North Pacific 61–66% of the time, compared to only 35% of the time for low SWE years (Fig. 6). Based on the air parcel trajectory positions above ground level (a.g.l.), high SWE years tend to have lower-level moisture transport, while for low SWE years the majority of the air is moving over Foy at higher elevations (>1500 m).

HYSPLIT 5-day air parcel back-trajectory analysis of anomalous SWE values based on the instrumental SWE record (1937–2011) (Pederson et al., 2011b). Individual years with **(a)** low SWE (n = 10) and **(b)** high SWE (n = 14) were identified over the period of available re-analysis data (1948–2019 NCEP-NCAR Reanalysis I (Kalnay et al., 1996)), and of these the 10 most recent high SWE years were chosen to provide an even comparison of total number of trajectories. The air parcel back-trajectories show that in high SWE years there are ~45 more snow days than the low SWE years, a 22% increase on average.

3.4. *Preliminary 2200 year lake sediment δ^{18}O SWE reconstruction*

The extended ~2200-year April 1 SWE reconstruction from the lake sediment δ^{18}O record was successfully calibrated against the tree-ring based NRM-SWE reconstruction, providing a long-term context in which to interpret the 20th century northern Rocky Mountain SWE declines (Fig. 7). The reconstruction model describes 32% of the variability in the tree-ring based NRM-SWE reconstruction target over the time period from 1252 to 1992 C.E. The reconstruction cross-validation statistics for the models calibrated on the first and second halves of the NRM-SWE record respectively were; Verification $R^2 = 0.24$ and 0.39, Reduction of Error (RE) = 0.16 and 0.34, and Coefficient of efficiency (CE) = 0.16 and 0.33. Positive values for RE and CE suggest the models calibrated on either half of the tree-ring NRM-SWE record provide skillful predictions of SWE over the validation period and capture long-term shifts in NRM-SWE means. The resolution of the δ^{18}O-based April 1 SWE reconstruction matches that of the original lake δ^{18}O record, roughly 5–7 years. Fig. 7 shows the 20-year spline of the lake δ^{18}O April 1 SWE reconstruction bounded by 95% prediction intervals and plotted alongside the smoothed and binned tree-ring based NRM-SWE reconstruction.

The new lake δ^{18}O April 1 SWE reconstruction extends the tree-ring based NRM-SWE reconstruction by ~1400 years, and captures first millennium decadal to centennial-scale variability in regional snowpack that was perhaps greater in magnitude (i.e. spectral power) than second millennium SWE variability (Fig. 7a). With the exception of several severe snow droughts occurring between ~400 and 700 C.E., the first millennium was defined by generally sustained high SWE conditions of equal to greater magnitude than occurred during the Little Ice Age (LIA ~1400–1850 C.E.). The Medieval Climate Anomaly (MCA ~800–1200 C.E.) is shown to be a period of average to below average snowpack conditions punctuated by several decadal-scale high and low snowpack anomalies. Numerous severe SWE droughts are evident throughout the record, with decadal-scale snow droughts becoming more commonplace in the second millennia. The major snow droughts occurring between approximately 400−650 C.E. and 1400 C.E rivaled modern snow droughts of the 1930s (i.e. the Dust Bowl Drought) and after the 1980s (Fig. 7b).

4. Discussion

In this work, we have successfully developed and demonstrated methods for the statistical calibration of a high-resolution lake sediment record to a tree-ring based snowpack reconstruction. Our innovative approach improved the accuracy of the lake sediment record depth-age model (Fig. 3), quantitatively identified the dominant hydroclimate sensitivity of the carbonate oxygen isotope ratios (Figs. 4–6), and allowed for the calibration of a lake sediment isotope chronology to modern snowpack variability, enabling the production of a multi-millennial δ^{18}O-based SWE reconstruction (Fig. 7b). These methods and robust results show the potential for future quantitative paleoclimatic reconstructions made possible by combining high-resolution sediment records with tree-ring records where they co-occur. The quantitative approach presented here also motivates a reexamination of existing δ^{18}O lake records, and the implementation of similar techniques for the future development of robust sediment-derived paleoclimate reconstructions.

It is important to reiterate that the approach presented here requires high-resolution lake records (annual to sub-decadal). This is because processes of both dating correction and statistical calibration rely on the common expression of climate-associated variability in tree-ring and lake records. In western North America, characteristics of climate system forcings responsible for variability in snowpack, streamflow, and drought exhibit maximum power in 3–7 year and 14–20+ year periodicities (Pederson et al., 2011b; Ault et al., 2013; Gangopadhyay et al., 2019), which aligns well with the strongest decadal-scale common signals of co-variability shown in the lake sediment and tree-ring snowpack reconstructions (Fig. 7a). While variability defined by 3–7 year cycles would be difficult to detect in the highest resolution lake records, even variability occurring on decadal to bi-decadal cycles likely requires lake records with roughly a 5-year resolution or higher to adequately capture the total magnitudes of such modes of variability. Accordingly, identification of lakes and implementation of sampling designs that allow for high temporal resolution in lake proxy records is critical for the successful implementation of this approach.

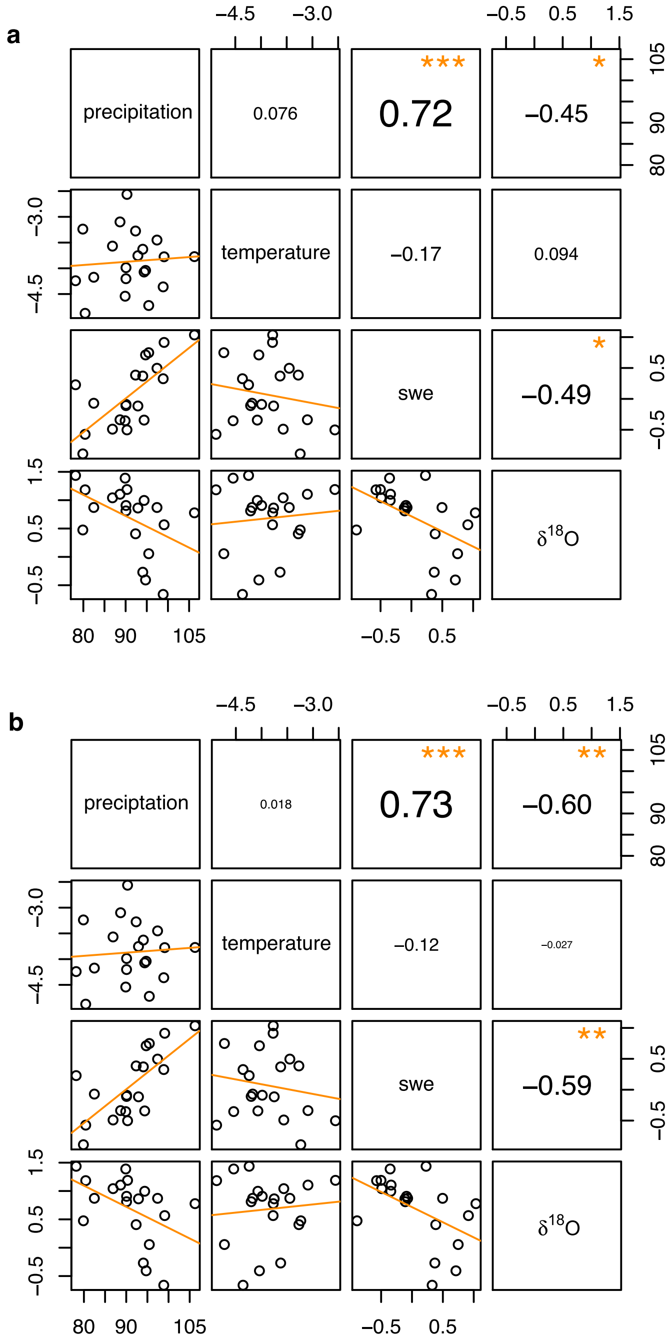

Fig. 5. Instrumental period climate correlations. (a) Correlations between 5-year binned precipitation, temperature, snow water equivalent (SWE), and Foy Lake sediment $\delta^{18}O$ based on Pearson's correlation coefficient, and **(b)** Spearman's rank correlation coefficient. Correlation p-values are indicated by stars such that for * $p < 0.05$, ** $p < 0.01$, and ***$p < 0.001$. Orange lines show the best fit for the pairwise relationships determined by ordinary least squares regression irrespective of correlation measure.

4.1. Insights from modern relationships between northern Rocky Mountain hydroclimate and Foy Lake $\delta^{18}O$

The novel methodological approaches used here improve the accuracy of the sediment age-dating by cross-correlating to the decadal-scale variations of the tree-ring based SWE records and greatly improve the potential for climatic interpretation of the Foy Lake sediment record. To anchor our climatic interpretation to the modern era, we correlated the lake $\delta^{18}O$ to observation-based estimates of precipitation, temperature and SWE over the period of overlap, which provided important insight into the present-day climate controls on isotopic values in the sediment record. These results then enabled an understanding of the mechanisms driving the shared variability between records and underpinned the statistical basis for reconstructing SWE from lake $\delta^{18}O$.

Based on the strong modern relationship between NRM-SWE and Foy Lake $\delta^{18}O$, it is apparent that winter snowpack input into the lake system strongly influences the observed variability in $\delta^{18}O$ (Figs. 4 and 5). Some degree of evaporative enrichment of lake waters is also evident in the position of Foy Lake waters to the right of the global meteoric water line (GMWL) in $\delta^{18}O$ – δD space (see Fig. 2 in Anderson et al. (2016b)). However, the relatively strong correlation between snowpack and lake $\delta^{18}O$, and weaker relationship between air temperature and lake $\delta^{18}O$, suggest that the effect of evaporation on lake $\delta^{18}O$ is likely secondary to the effect of snowpack over time.

These findings could be viewed as contrary to the typical interpretation that enriched lake waters indicate a lake-system dominated by evaporation (e.g., Shapley et al., 2009; Steinman et al., 2010, 2012; Steinman and Abbott, 2013; Steinman et al., 2014; Anderson et al., 2016b). However, it is important to recognize that, in order for even highly enriched lake waters to serve as precipitation/snowpack isometers, it is only necessary that the sensitivity of lake $\delta^{18}O$ to variability in inflow characteristics (magnitude, timing, inflow chemistry) is greater than the sensitivity of lake $\delta^{18}O$ to variability in evaporation-season temperature over time. At least in the case of the Foy Lake $\delta^{18}O$ record, we show that the sub-decadal through centennial-scale variability in the lake water isotopic composition is strongly controlled by temporal variability in snowpack (Figs. 4, 5 and 7). This signal is then preserved during the precipitation of carbonate which typically occurs in early summer, prior to strong evaporative enrichment during late summer months. The strong relationships shown between precipitation, SWE, and $\delta^{18}O$ in the Pend-Oreille watershed demonstrates that cool-season precipitation is a primary driver of SWE and lake $\delta^{18}O$, whereas temperature exerts a minor secondary influence on both SWE and lake $\delta^{18}O$ (Fig. 5). Considered together, these findings demonstrate why the approach presented here provides a robust reconstruction of snowpack using Foy Lake oxygen isotopes. First, these findings show that air temperature is not a large contributor to variability in the lake $\delta^{18}O$ snowpack proxy over time and; second, they show that the impact of air temperature on regional snowpack variability is generally integrated into the lake chemistry as snowpack melt drives variability in characteristics of lake inflow. These new findings highlight the need for further study to refine our understanding of lake $\delta^{18}O$ as a climate proxy in snow-driven systems. Our results also demonstrate that the improved dating accuracy afforded by the use of tree rings for dating corrections provides new opportunities for robust snowpack, lake $\delta^{18}O$ comparisons.

The multi-millennial quantitative reconstruction of April 1 SWE produced from the high-temporal resolution Foy Lake carbonate isotope ratios is noteworthy in that without adjustment of the sediment depth-age scale via annually dated tree-ring records, the modern calibration to historical climate variables would have been impossible. Traditionally, most lake sediment records use the date of extraction as the date for the top sample of the core and then select either bulk sediments at evenly spaced intervals or terrestrial macrofossils where available for radiocarbon dating. Due to the relatively high cost of radiometric dating and the considerable length of records, sediments are sampled at larger intervals (e.g., 25–30 cm) to obtain 3-4 ages per meter. The resulting age-model is produced by fitting a linear, polynomial, or Bayesian function to the depth-age data over spans of thousands of years for the entire record. In some longer cores, there may be only one date per thousand years, as is the case with the Foy Lake core. The limitation of this approach is that less attention is paid to the upper sediments spanning the historical period, which is required for robust calibration to modern climate data.

Calibration to the modern climate data is possible if the sediment core

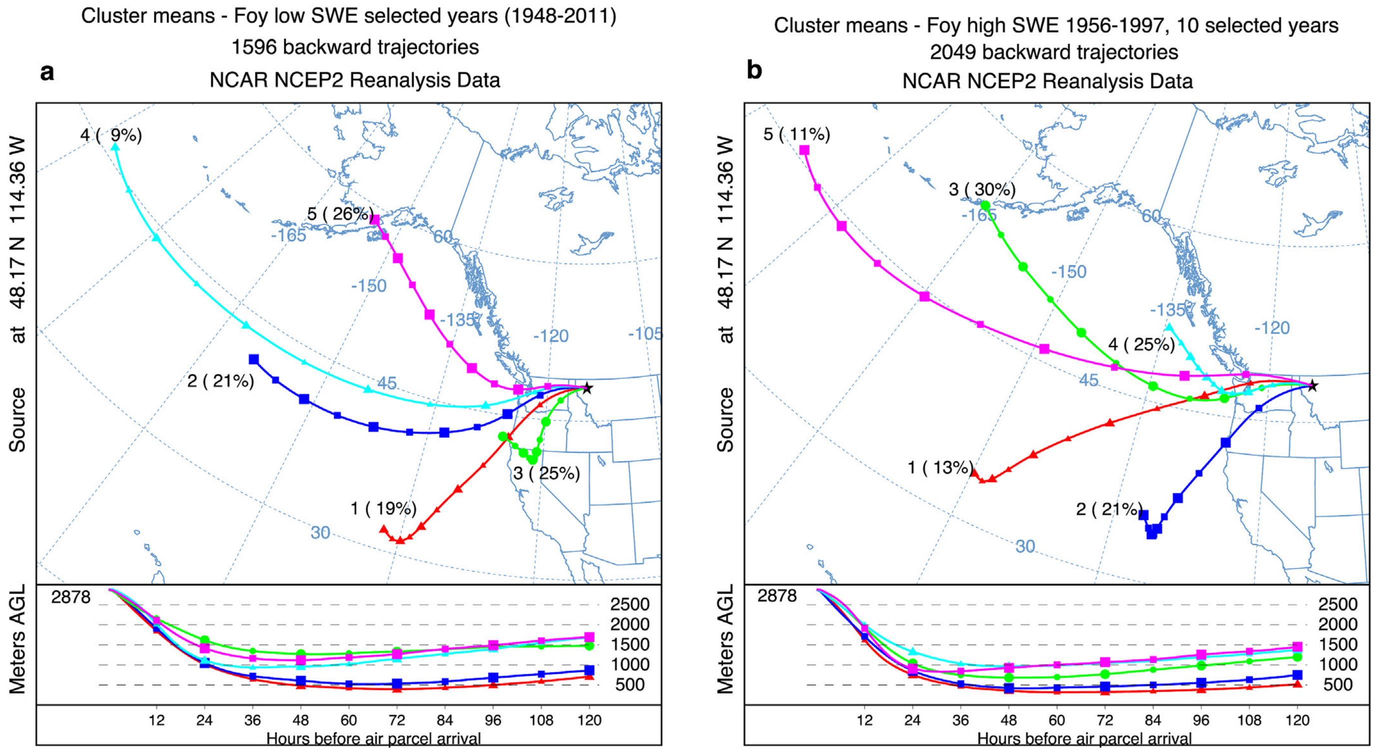

Fig. 6. Back-trajectory analysis of instrumental SWE record.

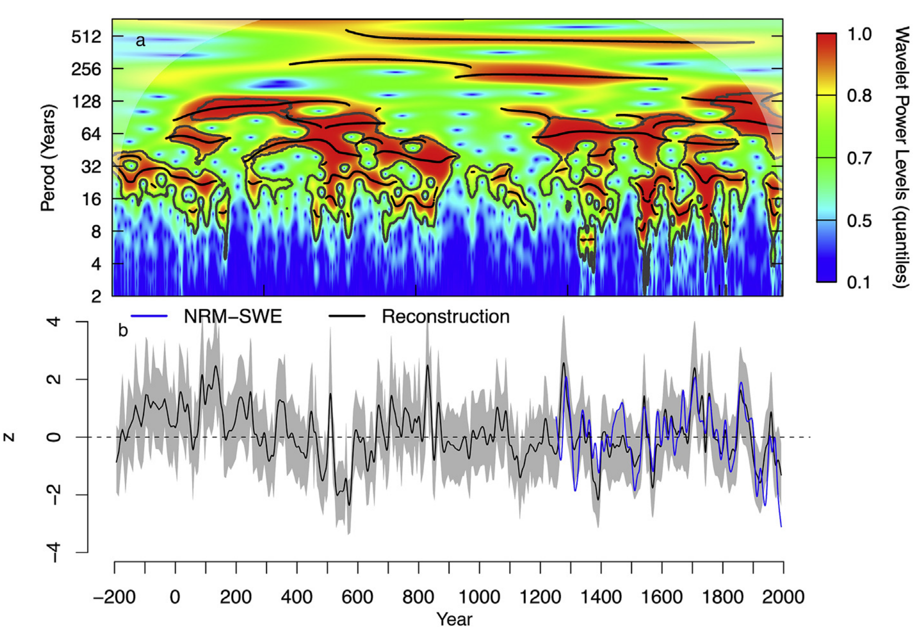

Fig. 7. Lake sediment-based northern Rockies snowpack reconstruction and spectral analyses. (a) Global average wavelet spectrum shows significant and increasing power throughout the timeseries between 10 and 128 year frequencies, and periods of significant power at frequencies > 128 years. **(b)** The 2200-year reconstruction of Northern Rocky Mountains Snow Water Equivalent (NRM-SWE) based on Foy Lake sediment δ^{18}O. Gray shading indicates the 95% prediction interval for the reconstruction. Values shown are the 20-year spline of the ~5-year resolution reconstruction that has been interpolated to annual resolution using a linear interpolation approach.

has a high-sedimentation rate and is sampled at high-frequency (e.g., 0.5 cm for ~10–20 dates per century), but even so, if the upper age-model is poorly constrained the data may result in weak correlation. Radiogenic lead ^{210}Pb dating of sediment has been used to improve modern chronologies, but can be erroneous or less reliable due to large scale disturbance of sediments and/or the watershed (Baskaran et al., 2014). Using our approach, the signal matching between the upper sediment δ^{18}O and historical tree-ring based SWE allowed for fine-tuning of the varve-counted age-model and therefore greatly improved the correlations to observed climate records. The novelty of the methodological approach used here is the critical link that the tree-ring chronologies provide between the observed SWE (i.e., snowcourse and SNOTEL data) and long-term lake δ^{18}O reconstructed SWE. Considering these records in concert allows for the statistical calibration and verification to modern climate variables over the much longer period of shared overlap between the paleorecords (~750 years).

4.2. Atmospheric controls on northern Rocky Mountain hydroclimate and Foy Lake δ^{18}O

To better understand the broader atmospheric dynamics driving the modern variability of SWE, and thus lake δ^{18}O, we employed the

HYSPLIT air parcel back-trajectory model. The air parcel back-trajectory analysis of the modern reanalysis data for high/low SWE years identified general atmospheric circulation patterns that are common in the northern Rockies. Although the SWE reconstruction itself is derived from a single location (Foy Lake), the spatial extent of the tree-ring calibration covers the entire NRM region and therefore should be reasonably representative of the region due to the spatial homogeneity of ocean-atmosphere teleconnected climate dynamics (e.g., El Niño Southern Oscillation (ENSO), Pacific Decadal Oscillation (PDO), and Aleutian Low (AL)).

In high SWE years, moisture sources typically originated in the far North Pacific (~65% of the time) (Fig. 6), which aligns with the negative phase of the Pacific Decadal Oscillation (PDO−) flow from the North Pacific high and British Columbia low, pulling moisture southward out of the North Pacific and into a low pressure environment in the Pacific Northwest (PNW), leading to greater winter storms and snowfall. In contrast, the larger southerly flow component in the low SWE years aligns more closely with the PDO+ and/or El Niño atmospheric patterns and the associated blocking high over the PNW (Pederson et al., 2011b). The height of trajectory pathways show that in low-SWE years, the majority of air masses are passing over Foy at higher atmospheric levels (>1500 m a.g.l) as compared with trajectory heights observed during high-SWE years (<1500 m a.g.l) (Fig. 6). Low SWE years are typically characterized by warmer water off the west coast, lower surface albedo on land, and persistent high pressure over the PNW, all of which generate surface high pressure that displaces incoming moisture higher into the atmosphere (Pederson et al., 2011b). The displacement of moisture higher in the atmosphere over the Foy Lake region in general could be indicative of lift that has already occurred to the west which would have likely caused prior distillation and rainout of moisture bearing air masses. This could also lead to lower precipitable water in colder air aloft and a reduced orographic effect (Luce et al., 2013) resulting in reduced precipitation in the mountains above Foy Lake during low SWE years.

In this first effort to combine lake- and tree-based proxy records, we did not quantify the potential effect of dominant moisture source region on lake sediment $\delta^{18}O$. However, it is possible that differences in dominant storm trajectories from one year to the next may impart an isotopic signal on regional snowpacks and lake sediments alike (Anderson, 2012). Understanding if and how this process occurs would widen the application of lake sediment isotope records as climate proxies in the future. Nonetheless, the strong interannual correlation between SWE and lake sediment $\delta^{18}O$ despite changes in dominant storm trajectories from year to year demonstrates that any such effect on the isotopic signal in the lake record is likely strongly secondary to the simple volume of snow melt water delivered to the lake each year.

4.3. Long-term context of current SWE declines

Snowpack reconstructions spanning the last 800 years have been produced from tree-rings for the northern Rocky Mountains (Pederson et al., 2011a), and have now been extended an additional 1400 years through the first millennium by calibrating lake sediment $\delta^{18}O$ to tree-ring based April 1 SWE reconstructions (Fig. 7b). Differences in snowpack variability are evident between millennia, with much of the first millennium defined by generally high snowpack conditions apart from a handful of notable severe and long-duration snow megadroughts between ~400 and 650 C.E. To clarify, definitions of megadrought vary, but here we use the term megadrought to refer to multidecade drought events that are of long duration (>20 years) (e.g., Williams et al., 2020). In contrast, the second millennium exhibits variability in high and low snowpack anomalies that are generally shorter in duration (Fig. 7a). The existing tree-ring based SWE reconstruction extends to 1250 C.E., which captured the LIA period (~1400–1850 C.E.) of generally elevated SWE, but ended just short of the MCA (~800–1200 C.E.). In Fig. 7b, the $\delta^{18}O$-based reconstruction shows generally below average SWE conditions throughout the MCA punctuated by only a few above average SWE anomalies. Remarkably, the period of positive SWE anomalies from ~-150 to 250 C.E. were likely longer in duration and potentially greater in magnitude than the snowpack conditions during the LIA.

Regarding severe snow droughts and comparisons to recent snowpack conditions, over the entire reconstruction there are only a few decadal periods where negative SWE anomalies reach similar magnitudes as SWE declines occurring in recent decades (Fig. 7b). A number of notable snow megadroughts relative to modern conditions are evident in the record including ~475–500 C.E., ~525–575 C.E., ~1100–1200 C.E., ~1350–1400 C.E. and ~1550–1580 C.E (Fig. 7b). The major snow droughts occurring between approximately 400−650 C.E. and around 1400 C.E exhibit magnitudes similar to modern snow drought intensities of the Dust Bowl Drought (1930s) and the recent Turn-of-the-Century Drought (2000s) (Pederson et al., 2011b; Mote et al., 2018). During the MCA period, the negative SWE anomalies are generally relatively modest but show a sustained period of snow drought from ~1100 to 1200 C.E. Of equal importance to snow drought events is that the 20th century high SWE anomalies are considerably lower (approximately half) on average than substantial portions of the entire two millennia SWE reconstruction. The key conclusion here is that the 20th century baseline, as well as the current 30-yr normal (1981–2010), likely represents a highly negative departure from the long-term average snowpack conditions of the northern Rocky Mountains. As such, continued declines in snowpack beyond those observed during the 20th and early 21st century would push future average snowpack conditions well outside the range of variability experienced by Northern Rocky Mountain ecosystems over the last two millennia.

4.4. New insights and future research using combined lake sediment – tree ring paleoclimate reconstructions

The development of this novel method raises new questions. Here we discuss some of the potential challenges with using this approach followed by important research needs.

Results from the Foy Lake isotope record suggest it may not be possible to predict a particular lake's climate sensitivity from in-situ chemistry alone (e.g., conductivity, alkalinity, or water isotope composition), which is common practice in modern lake sediment paleoclimate studies (e.g., Leng and Anderson, 2003; Leng and Marshall, 2004; Steinman and Abbott, 2013; Jones et al., 2016b; Bowen et al., 2018). Rather, researchers need well-dated, highly-resolved lake sediment values (e.g., carbonate isotopes, diatom/pollen/charcoal concentrations, etc.) that can be compared with appropriate climate records to determine proxy-climate relationships. Thus, in order to more broadly apply these methods, future research should target the development of high-resolution lake records (i.e., high sedimentation rates and/or high-frequency sampling) extending to present-day if possible. Additionally, high dating accuracies over the common multi-century period of overlap with the tree-ring based climate reconstructions are necessary to calibrate lake-sediment based climate reconstructions. In the case of the Foy Lake record, the average resolution of ~5–7 years per sample was sufficient, whereas records with less than 0.3 mm/year (~15 years per ½ cm sample) may not provide a high enough resolution for statistical analyses. Each of these aspects appear critical for establishing accurate dating against tree-ring records and the calibration process to modern climate variables.

Obvious major questions raised by these requirements include: 1) how well will this approach work for other proxies with theoretical links to lake sediment $\delta^{18}O$ – like formation temperature or evaporation?; 2) what lake sites and associated site characteristics should be targeted for reconstruction of different climate variables?; and 3) what is the overall potential for this work to be replicated? Much of the historical approach of interpreting lake sediment isotope signals has been based on producing co-isotope plots of hydrogen and oxygen from lake-water samples along the LMWL and comparing them to modern precipitation to determine the lake's hydrologic balance. However, limitations of this approach prevent the capture of information contained in the lake's decadal-to centennial-scale isotopic variability, and the correlation (or lack thereof) to relevant climate signals. The novel and quantitative findings presented here represent a first and early step forward in this regard, and rather than providing a definitive answer to these questions, calls for renewed examination of the hydroclimatic drivers of both modern and long-term sediment $\delta^{18}O$ variability. Further research potential may already exist in a number of existing or candidate sediment records from lakes with sufficient in-situ carbonate concentration, elevated sedimentation rates, reasonable residence times, and persistent lake levels over time. In Montana alone, there are a number of lake sediment records (~10–20) within the LacCore database (published & unpublished) where the application of this approach may be feasible.

5. Conclusion

In this research, we have presented a novel approach for the development of a quantitative, multi-millennial snowpack reconstruction based upon the calibration of a high-resolution lake sediment record to a tree-ring based April 1 SWE reconstruction. We also extend previous reconstructions of SWE by ~1400 years. Matching decadal scale $\delta^{18}O$ signals with annually dated tree-ring based SWE signals greatly improved the accuracy of the lake sediment record depth-age model. Statistical correlation of the age-adjusted sediment $\delta^{18}O$ record to modern climate data then quantitatively identified the hydroclimate sensitivity of the carbonate oxygen isotope ratios. These innovative methods and robust preliminary results illustrate the potential for developing future quantitative paleoclimatic reconstructions using high-resolution sediment records in combination with tree-ring records. Furthermore, the analytical approach presented here motivates a closer look at how previous sediment $\delta^{18}O$-climate relationships have been inferred, underscoring the need for implementing rigorous calibration of sediment proxy records to modern climate records for the development of robust sediment-derived paleoclimate reconstructions.

The long-term context afforded by the SWE reconstruction demonstrates previously unseen multi-centennial snowpack dynamics and provides a new perspective on the end-of-century (i.e., post-1980s) snow drought. There is a remarkable low frequency signal in the reconstruction showing strong trends and persistent anomalies in SWE of up to 500 years (e.g. 100–600 C.E.) (Fig. 7a). Linking such observations in snowpack to potential climate drivers will require new climate proxies of similar resolution and temporal extent that have the ability to preserve signals associated with slowly varying climate processes. The long-term record presented here indicates that the northern Rockies have recently entered a new low-snow phase around 1900 after ~300 years of fairly high-snow conditions. Considering this shift, and the current trajectory of climate warming impacts, it is plausible that low-snow conditions have indeed become the new climatic norm.

The severe snow drought around 500–600 C.E. is similar to the previous acute declines in observed SWE, but is remarkable in that this event lasted nearly 100 years, much longer than other extreme events. This suggests there is an earlier precedent for the recent snowpack declines at least through 2000 C.E. However, the magnitude of regional snowpack declines over the last two decades of the 20th century may well have surpassed the low SWE levels of the 500–600 C.E. megadrought (Mote et al., 2018). Given this new long-term perspective and future projections for continued warming-induced snowpack declines in the region (Larson et al., 2011; MacDonald et al., 2011) it is reasonable to view the recent snowpack declines as a 'severe snow drought'. In terms of severity, the most recent decades of the record are as dry as any in the last 2200 years, with great ecological and social consequences. Future efforts to better understand the relationship between recent changes in snowpack and long-term climate variability will be critical for managing potentially scarce water resources into the future.

Author contributions

SWS, JTM, GTP, and DBM conceived the study. SWS, JTM and GTP designed and performed the analyses and visualizations. JTM managed and prepared data, implemented software. GTP provided data. SWS, JTM, and GTP wrote the manuscript; DBM reviewed and provided edits to manuscript drafts.

Data availability

The observed, tree-ring, and lake sediment based April 1 SWE reconstructions are available from NOAA National Centers for Environmental Information (NCEI) Paleoclimate database. Available here: https://www.ncdc.noaa.gov/paleo/study/30632.

Declaration of competing interest

The authors declare that they have no known competing financial interests or personal relationships that could have appeared to influence the work reported in this paper.

Acknowledgments

We thank Angela DesJardins for her support of this study. This research was supported by the NASA Montana Space Grant Consortium [grant number NNX15AJ19H]; DBM was partially supported by National Science Foundation [grant numbers BCS-1539820, BCS-1832486]. GTP and JTM were supported by the U.S. Geological Survey North Central Climate Adaptation Science Center, and the Land Resources and Ecosystems Mission Areas. Any use of trade, firm, or product names is for descriptive purposes only and does not imply endorsement by the U.S. Government.

References

Anderson, L., 2012. Rocky mountain hydroclimate: Holocene variability and the role of insolation, ENSO, and the north American monsoon, *global planet.* Change 92–93, 198–208. https://doi.org/10.1016/j.gloplacha.2012.05.012.

Anderson, L., Brunelle, A., Thompson, R.S., 2015a. A multi-proxy record of hydroclimate, vegetation, fire, and post-settlement impacts for a subalpine plateau, central Rocky Mountains. U.S.A, *The Holocene* 25 (6), 932–943. https://doi.org/10.1177/0959683615574583.

Anderson, L., Berkelhammer, M., Mast, M.A., 2016a. Isotopes in north American Rocky mountain snowpack 1993–2014. Quat. Sci. Rev. 131, 262–273. https://doi.org/10.1016/j.quascirev.2015.03.023.

Anderson, L., Berkelhammer, M., Barron, J.A., Steinman, B.A., Finney, B.P., Abbott, M.B., 2016b. Lake oxygen isotopes as recorders of North American Rocky Mountain hydroclimate: Holocene patterns and variability at multi-decadal to millennial time scales, *Global Planet.* Change 137, 131–148. https://doi.org/10.1016/j.gloplacha.2015.12.021.

Anderson, L., Berkelhammer, M., van Sistine, P., Mast, A., Ingersoll, G., Clow, D., 2015b. A spatiotemporal network of isotopes in Rocky Mountain Snowpack. Quat. Int. 387 (C), 132. https://doi.org/10.1016/j.quaint.2015.01.126.

Ault, T.R., Cole, J.E., Overpeck, J.T., Pederson, G.T., St George, S., Otto-Bliesner, B., Woodhouse, C.A., Deser, C., 2013. The continuum of hydroclimate variability in western North America during the last millennium. J. Clim. 26 (16), 5863–5878. https://doi.org/10.1175/JCLI-D-11-00732.1.

Bales, R.C., Molotch, N.P., Painter, T.H., Dettinger, M.D., Rice, R., Dozier, J., 2006. Mountain hydrology of the western United States. Water Resour. Res. 42 (8), 303–313. https://doi.org/10.1029/2005WR004387.

Barandiaran, D., Wang, S.Y., DeRose, R., 2017. Gridded snow water equivalent reconstruction for Utah using forest inventory and analysis tree-ring data. Water 9 (403), 1–13. https://doi.org/10.3390/w9060403.

Barnett, T.P., et al., 2008. Human-induced changes in the hydrology of the western United States. Science 319 (5866), 1080–1083. https://doi.org/10.1126/science.1152538.

Baskaran, M., Nix, J., Kuyper, C., Karunakara, N., 2014. Problems with the dating of sediment core using excess 210Pb in a freshwater system impacted by large scale watershed changes. J. Environ. Radioact. 138 (c), 355–363. https://doi.org/10.1016/j.jenvrad.2014.07.006.

Belmecheri, S., Babst, F., Wahl, E.R., Stahle, D.W., Trouet, V., 2015. Multi-century evaluation of Sierra Nevada snowpack. Nat. Clim. Change 6 (1), 2–3. https://doi.org/10.1038/nclimate2809.

Berkelhammer, M., Stott, L.D., 2012. Secular temperature trends for the southern Rocky Mountains over the last five centuries. Geophys. Res. Lett. 39 (L17701), 1–6. https://doi.org/10.1029/2012GL052447.
Bershaw, J., Penny, S.M., Garzione, C.N., 2012. Stable isotopes of modern water across the Himalaya and eastern Tibetan Plateau: implications for estimates of paleoelevation and paleoclimate. J. Geophys. Res. 117 (D02110), 1–18. https://doi.org/10.1029/2011JD016132.
Bohr, G.S., Aguado, E., 2001. Use of April 1 SWE measurements as estimates of peak seasonal snowpack and total cold-season precipitation. Water Resour. Res. 37 (1), 51–60.
Bowen, G.J., Putman, A., Brooks, J.R., Bowling, D.R., Oerter, E.J., Good, S.P., 2018. Inferring the source of evaporated waters using stable H and O isotopes. Oecologia 1–15. https://doi.org/10.1007/s00442-018-4192-5.
Box, G.E.P., Cox, D.R., 1964. An analysis of transformations. J. Roy. Stat. Soc. B 26 (2), 211–243. https://doi.org/10.1111/j.2517-6161.1964.tb00553.x.
Briffa, K.R., Jones, P.D., Pilcher, J.R., Hughes, M.K., 1998. Reconstructing summer temperatures in northern Fennoscandia back to AD 1700 using tree-ring data from Scots Pine. Arct. Alp. Res. 20 (4), 385–394. https://doi.org/10.1080/00040851.1988.12002691.
Briffa, K.R., Osborn, T.J., Schweingruber, F.H., Jones, P.D., Shiyatov, S.G., Vaganov, E.A., 2002. Tree-ring width and density data around the Northern Hemisphere: Part 1, local and regional climate signals. Holocene 12 (6), 737–757. https://doi.org/10.1191/0959683602hl587rp.
Brunelle, A., Minckley, T.A., Lips, E., Burnett, P., 2013. A record of Lateglacial/Holocene environmental change from a high-elevation site in the Intermountain West, USA. J. Quat. Sci. 28 (1), 103–112. https://doi.org/10.1002/jqs.2600.
Chellman, N., McConnell, J.R., Arienzo, M., Pederson, G.T., Aarons, S.M., Csank, A., 2017. Reassessment of the upper Fremont Glacier ice-core chronologies by synchronizing of ice-core-water isotopes to a nearby tree-ring chronology. Environ. Sci. Technol. 51 (8), 4230–4238. https://doi.org/10.1021/acs.est.6b06574.
Cook, E.R., Kairiukstis, L.A., 1990. Methods of Dendrochronology: Applications in the Environmental Sciences. Springer Netherlands, Dordrecht.
Dorfman, R.A., 1938. A note on the delta-method for finding variance formulae. Biometrics Bull. 1, 129–138.
Douglass, E.A., 1935. Dating Pueblo Bonito and Other Ruins of the Southwest. National Geographic Society.
Evans, M.N., Tolwinski-Ward, S.E., Thompson, D.M., Anchukaitis, K.J., 2013. Applications of proxy system modeling in high resolution paleoclimatology. Quat. Sci. Rev. 76, 16–28. https://doi.org/10.1016/j.quascirev.2013.05.024.
Fritts, H.C., 1976. Tree Rings and Climate. Academic Press, New York, USA.
Gangopadhyay, S., McCabe, G., Pederson, G., Martin, J., Littell, J.S., 2019. Risks of hydroclimatic regime shifts across the western United States. Sci. Rep. 9 (1), 1–8. https://doi.org/10.1038/s41598-019-42692-y.
Gray, S.T., Graumlich, L.J., Betancourt, J.L., 2017. Annual precipitation in the yellowstone National Park region since AD 1173. Quaternary Research 68 (1), 18–27. https://doi.org/10.1016/j.yqres.2007.02.002.
Harpold, A.A., Dettinger, M.D., Rajagopal, S., 2017. Defining snow drought and why it matters. Eos 98, 1–5. https://doi.org/10.1029/2017EO068775.
Harpold, A., Brooks, P., Rajagopal, S., Heidbuchel, I., Jardine, A., Stielstra, C., 2012. Changes in snowpack accumulation and ablation in the intermountain west. Water Resour. Res. 48 (W11501), 1–11. https://doi.org/10.1029/2012WR011949.
Jones, M.D., Cuthbert, M.O., Leng, M.J., McGowan, S., Mariethoz, G., Arrowsmith, C., Sloane, H.J., Humphrey, K.K., Cross, I., 2016a. Comparisons of observed and modelled lake d18O variability. Quat. Sci. Rev. 131, 329–340. https://doi.org/10.1016/j.quascirev.2015.09.012.
Jones, M.D., Dee, S., Anderson, L., Baker, A., Bowen, G., Noone, D.C., 2016b. Water isotope systematics: improving our palaeoclimate interpretations. Quat. Sci. Rev. 131, 243–249. https://doi.org/10.1016/j.quascirev.2015.11.014.
Kalnay, E., Kanamitsu, M., Kistler, R., Collins, W., Deaven, D., Gandin, L., Iredell, M., Saha, S., White, G., Woollen, J., 1996. The NCEP/NCAR 40-year reanalysis project. Bull. Am. Meteorol. Soc. 77 (3), 437–471.
Larson, R.P., Byrne, J.M., Johnson, D.L., Kienzie, S.W., Letts, M.G., 2011. Modelling climate change impacts on spring runoff for the Rocky mountains of Montana and alberta II: runoff change projections using future scenarios. Can. Water Resour. J. 36 (1), 35–52. https://doi.org/10.4296/cwrj3601035.
Leng, M.J., Anderson, N.J., 2003. Isotopic variation in modern lake waters from western Greenland. Holocene 13 (4), 605–611. https://doi.org/10.1191/0959683603hl620rr.
Lisiecki, L.E., Lisiecki, P.A., 2002. Application of dynamic programming to the correlation of paleoclimate records. Paleoceanography 17 (4). https://doi.org/10.1029/2001PA000733, 1–1–1–12.
Luce, C.H., Abatzoglou, J.T., Holden, Z.A., 2013. The missing mountain water: slower westerlies decrease orographic enhancement in the Pacific Northwest USA. Science 342. https://doi.org/10.1126/science.1245095.
Lundeen, Z., Brunelle, A., Burns, S.J., Polyak, V., Asmerom, Y., 2013. A speleothem record of Holocene paleoclimate from the northern Wasatch Mountains, southeast Idaho, USA. Quat. Int. 310, 83–95. https://doi.org/10.1016/j.quaint.2013.03.018.
Lundquist, J.D., Dettinger, M.D., Stewart, I.T., Cayan, D.R., 2008. Variability and trends in spring runoff in the western United States. In: Waggoner, F. (Ed.), Climate Warming in Western North America: Evidence and Environmental Effects. University of Utah Press, Salt Lake City, Utah, USA, pp. 63–76.
Lutz, E.R., Hamlet, A.F., Littell, J.S., 2012. Paleoreconstruction of cool season precipitation and warm season streamflow in the Pacific Northwest with applications to climate change assessments. Water Resour. Res. 48 (1) https://doi.org/10.1029/2011WR010687, 5875–16.
Leng, M.J., Marshall, J.D., 2004. Palaeoclimate interpretation of stable isotope data from lake sediment archives. Quat. Sci. Rev. 23 (7), 811–831.
MacDonald, R.J., Byrne, J.M., Kienzle, S.W., Larson, R.P., 2011. Assessing the potential impacts of climate change on mountain snowpack in the st. Mary river watershed, Montana. J. Hydrometeorol. 12 (2), 262–273. https://doi.org/10.1175/2010JHM1294.1.
Mote, P.W., Li, S., Lettenmaier, D.P., Xiao, M., Engel, R., 2018. Dramatic declines in snowpack in the western US. npj Climate and Atmospheric Science. https://doi.org/10.1038/s41612-018-0012-1, 2018 1:1, 1(1), 2.
Parnell, A.C., Buck, C.E., Doan, T.K., 2011. A review of statistical chronology models for high-resolution, proxy-based Holocene palaeoenvironmental reconstruction. Quat. Sci. Rev. 30 (21–22), 2948–2960. https://doi.org/10.1016/j.quascirev.2011.07.024.
Pederson, G.T., Gray, S.T., Woodhouse, C.A., Betancourt, J.L., Fagre, D.B., Littell, J.S., Watson, E., Luckman, B.H., Graumlich, L.J., 2011a. The unusual nature of recent snowpack declines in the north American cordillera. Science 333 (6040), 332–335. https://doi.org/10.1126/science.l204452.
Pederson, G.T., Gray, S.T., Ault, T., Marsh, W., Fagre, D.B., Bunn, A.G., Woodhouse, C.A., Graumlich, L.J., 2011b. Climatic controls on the snowmelt hydrology of the northern Rocky mountains. J. Clim. 24 (6), 1666–1687. https://doi.org/10.1175/2010JCLI3729.1.
Power, M.J., Whitlock, C., Bartlein, P.J., 2011. Postglacial fire, vegetation, and climate history across an elevational gradient in the Northern Rocky Mountains, USA and Canada. Quat. Sci. Rev. 30 (19–20), 2520–2533. https://doi.org/10.1016/j.quascirev.2011.04.012.
Power, M.J., Whitlock, C., Bartlein, P., Stevens, L.R., 2006. Fire and vegetation history during the last 3800 years in northwestern Montana. Geomorphology 75 (3–4), 420–436. https://doi.org/10.1016/j.geomorph.2005.07.025.
Prell, W.L., Imbrie, J., Martinson, D.G., Morley, J.J., Pisias, N.G., Shackleton, N.J., Streeter, H.F., 1986. Graphic correlation of oxygen isotope stratigraphy application to the Late Quaternary. Paleoceanography 1 (2), 137–162. https://doi.org/10.1029/PA001i002p00137.
Ramsey, C.B., 2008. Deposition models for chronological records. Quat. Sci. Rev. 27 (1–2), 42–60. https://doi.org/10.1016/j.quascirev.2007.01.019.
Shackleton, N.J., Hagelberg, T.K., Crowhurst, S.J., 1995. Evaluating the success of astronomical tuning: pitfalls of using coherence as a criterion for assessing pre-Pleistocene timescales. Paleoceanography 10 (4), 693–697. https://doi.org/10.1029/95PA01454.
Shapley, M.D., Ito, E., Donovan, J.J., 2009. Lateglacial and Holocene hydroclimate inferred from a groundwater flow-through lake, Northern Rocky Mountains, USA. Holocene 19 (4), 523–535. https://doi.org/10.1177/0959683609104029.
Sinclair, K.E., Marshall, S.J., Moran, T.A., 2011. A Lagrangian approach to modelling stable isotopes in precipitation over mountainous terrain. Hydrol. Process. 25 (16), 2481–2491. https://doi.org/10.1002/hyp.7973.
Stein, A.F., Draxler, R.R., Rolph, G.D., Stunder, B.J.B., Cohen, M.D., Ngan, F., 2015. NOAA's HYSPLIT atmospheric transport and dispersion modeling system. Bull. Am. Meteorol. Soc. 96 (12), 2059–2077. https://doi.org/10.1175/BAMS-D-14-00110.1.
Steinman, B.A., Abbott, M.B., 2013. Isotopic and hydrologic responses of small, closed lakes to climate variability: hydroclimate reconstructions from lake sediment oxygen isotope records and mass balance models. Geochem. Cosmochim. Acta 105 (C), 342–359. https://doi.org/10.1016/j.gca.2012.11.027.
Steinman, B.A., Abbott, M.B., Mann, M.E., Ortiz, J.D., Feng, S., Pompeani, D.P., Stansell, N.D., Anderson, L., Finney, B.P., Bird, B.W., 2014. Ocean-atmosphere forcing of centennial hydroclimate variability in the Pacific Northwest. Geophys. Res. Lett. 41 (7) https://doi.org/10.1002/(ISSN)1944-8007.
Steinman, B.A., Abbott, M.B., Mann, M.E., Stansell, N.D., Finney, B.P., 2012. 1,500 year quantitative reconstruction of winter precipitation in the Pacific Northwest. Proc. Natl. Acad. Sci. U. S. A 109 (29), 11619–11623. https://doi.org/10.1073/pnas.1201083109/-/DCSupplemental/Appendix.pdf.
Steinman, B.A., Rosenmeier, M.F., Abbott, M.B., Bain, D.J., 2010. The isotopic and hydrologic response of small, closed-basin lakes to climate forcing from predictive models: application to paleoclimate studies in the upper Columbia River basin. Limnol. Oceanogr. 55 (6), 2231–2245. https://doi.org/10.4319/lo.2010.55.6.2231.
Stevens, L.R., Stone, J.R., Campbell, J., Fritz, S.C., 2006. A 2200-yr record of hydrologic variability from Foy Lake, Montana, USA, inferred from diatom and geochemical data. Quaternary Research 65 (2), 264–274. https://doi.org/10.1016/j.yqres.2005.08.024.
Stokes, M.A., Smiley, T.L., 1968. An Introduction to Tree-Ring Dating. The University of Chicago Press.
Stone, J.R., Fritz, S.C., 2006. Multidecadal drought and Holocene climate instability in the Rocky mountains. Geology 34 (5), 409–412. https://doi.org/10.1130/g22225.1.
Westerling, A.L., Hidalgo, H.G., Cayan, D.R., Swetnam, T.W., 2006. Warming and earlier spring increase western U.S. Forest wildfire activity. Science 313 (5789), 940–943. https://doi.org/10.1126/science.1128834.
Whitlock, C., Marlon, J., Briles, C., Brunelle, A., Long, C., Bartlein, P., 2008. Long-term relations among fire, fuel, and climate in the north-western US based on lake-sediment studies. Int. J. Wildland Fire 17 (1), 72. https://doi.org/10.1071/WF07025.

Whitlock, C., Dean, W.E., Fritz, S.C., Stevens, L.R., Stone, J.R., Power, M.J., Rosenbaum, J.R., Pierce, K.L., Bracht-Flyr, B.B., 2012. Holocene seasonal variability inferred from multiple proxy records from Crevice Lake. Yellowstone National Park, USA, *Palaeogeography, Palaeoclimatology, Palaeoecology* 331–332, 90–103. https://doi.org/10.1016/j.palaeo.2012.03.001.

Williams, A.P., Cook, E.R., Smerdon, J.E., Cook, B.I., Abatzoglou, J.T., Bolles, K., Baek, S.H., Badger, A.M., Livneh, Ben, 2020. Large contribution from anthropogenic warming to an emerging North American megadrought. Science 368 (6488), 314–318. https://doi.org/10.1126/science.aaz9600.

Woodhouse, C.A., 2003. A 431-yr reconstruction of western Colorado snowpack from tree rings. J. Clim. 16 (10), 1551–1561. https://doi.org/10.1175/1520-0442(2003)016<1551:AYROWC>2.0.CO;2.